

Open Source Modeling of Heart Rhythm and Cardiac Pacing

Jie Lian*, Hannes Krätschmer and Dirk Müssig

Micro Systems Engineering, Inc., Lake Oswego, Oregon, USA

Abstract: *Background:* Despite the progress of cardiac arrhythmia research and the advance of the pacemaker technology, much remains unknown about how the external pacing interacts with the heart's intrinsic activity.

Methods: We present an open source computer model that is capable to simulate intrinsic heart rhythm under both normal and pathological conditions, and its interactions with extrinsic dual-chamber cardiac pacing. Detailed model structure and the software implementation are described.

Results: We demonstrate the usage of the computer model for generating realistic cardiac activation sequences under different rhythm conditions. Representative examples are also provided to illustrate the application of the model to evaluate the performance of pacing algorithms.

Conclusions: The present computer model provides a unified platform wherein it is possible to bench test advanced pacemaker algorithms in the presence of different heart rhythms. The availability of this open source model promises to support and stimulate future research in cardiac electrophysiology and development in pacemaker technology.

Keywords: Open source model, cardiac pacing, heart rhythm, pacemaker.

I. INTRODUCTION

The normal heart rhythm is maintained through a highly specialized electrical conduction system. The sinoatrial (SA) node serves as the natural pacemaker, generating rhythmic electrical pulses that spread across both atria. These electrical pulses are delayed at the atrio-ventricular (AV) junction (or AVJ), then travel along left and right bundle branches and excite both ventricles (Fig. 1). Structural or functional abnormalities of the cardiac electrical conduction system can cause cardiac arrhythmias.

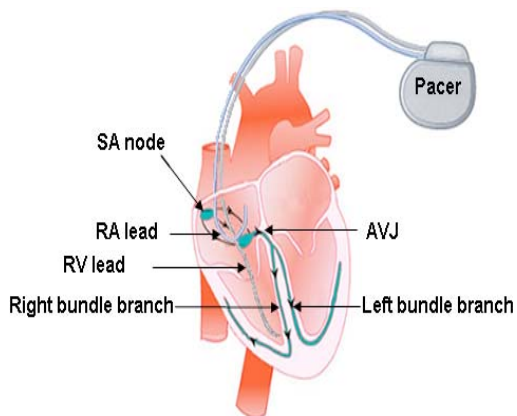


Fig. (1). Illustration of the cardiac electrical conduction pathway and an implantable dual-chamber cardiac pacemaker connecting with a right atrial lead and a right ventricular lead. Modified from [15] with permission (© 2008, Biomedical Engineering Society).

By delivering appropriately timed electrical impulses to the heart, the artificial cardiac pacemaker is a medical device that controls the heartbeat and treats various types of cardiac arrhythmia. The most commonly implanted pacemakers are dual-chamber pacemakers [1]. Connecting to a right atrial (RA) lead and a right ventricular (RV) lead, a dual-chamber pacemaker senses electrical signals in both right atrium and right ventricle, and paces one or both chambers when needed (Fig. 1).

Analysis of the heart rhythm can be challenging. Even in normal sinus rhythm, the cardiac inter-beat (RR) intervals fluctuate at various time scales, a phenomenon known as heart rate variability (HRV) [2]. In pathological conditions, puzzling patterns of heart rhythms can occur due to various cardiac disorders. More complexity is expected when involving cardiac pacing because of the interactions between intrinsic cardiac activation and extrinsic cardiac pacing. For instance, device sensing of intrinsic cardiac signal can inhibit the pacing, whereas device pacing may pre-excite the myocardium and suppress its intrinsic activity. When both intrinsic depolarization and paced depolarization are present, fusion beat is expected. On the other hand, despite the advance of pacemaker technology, modern pacemakers are far from fault-proof. Both under-sense (fail to detect cardiac activation) and over-sense (falsely detect cardiac activation) are not uncommon in pacemakers. Moreover, a pacing pulse may fail to depolarize the heart if the stimulation strength is below the physiological capture threshold, or if the heart is still refractory due to an earlier excitation.

In spite of the significant scientific merits and clinical importance, there is a stark paucity of computer models that can realistically simulate the interaction between intrinsic heart rhythm and cardiac pacing. During the past decades,

*Address correspondence to this author at the 6024 SW Jean Road, Lake Oswego, OR 97035, USA; Tel: 503-635-4016; Fax: 503-635-9610; E-mail: jie.lian@biotronik.com

tremendous efforts have been made to investigate the ventricular response in atrial fibrillation (AF), with particular focus on modeling of AV conduction [3-10]. Although these models may reasonably explain the irregular RR intervals in AF, cardiac pacing was not considered, and hence its effect on intrinsic rhythm could not be assessed.

Recently, two computer models have been developed to bridge the research gap. First, an AF-VP model was developed to elucidate the effects of ventricular pacing (VP) on ventricular rhythm in AF [11]. Computer simulations have shown that the AF-VP model could account for most experimental observations, including various patterns of RR interval histograms in AF, [11] biphasic relationship between atrial and ventricular rates in AF, [11] the rate smoothing effects of VP in AF, [11-13] and many well-known AV conduction and refractory properties [14]. Second, by incorporating more realistic heart rhythm generators, bi-directional wave conductions, and an industry-standard dual-chamber pacemaker timing control logic into the AF-VP model, we have developed an integrated dual-chamber heart and pacemaker (IDHP) model, which provides an abstract yet realistic representation of the native cardiac electrical conduction system and its interactions with external cardiac pacing [15].

To facilitate the use and further improvement of these computer models, their software programs have been respectively released in two prominent open source websites. The AF-VP model can be freely downloaded from the PhysioNet [http://www.physionet.org/physiotools/afvp/], [16] and recently the IDHP model has also been made freely available from the Physiome [http://nsr.bioeng.washington.edu/jsim/models/webmodel/NSR/NON_JSIM_MODELS/Li_an_Mussig_2009_IDHP/index.html] [17]. Moreover, the architecture and design of the AF-VP model have been provided in an open access format [18]. In a parallel effort, we describe in this open access paper the simulation framework, implementation, and application of the IDHP model.

II. MODEL STRUCTURE

We use a system modeling approach to simulate the interactions between intrinsic heart activity and extrinsic cardiac pacing. Fig. 2 shows the schematic diagram of the IDHP model structure, which consists of 8 inter-connected modules: (1) atrial rhythm generator (ARG), (2) ventricular rhythm generator (VRG), (3) RA conductor, (4) RV conductor, (5) AVJ, (6) RA lead, (7) RV lead, and (8) pacer. By constructing 8 inter-connected modules, we are able to encapsulate electrophysiological properties of the heart and detailed pacemaker control logics into one integrated system. Such a modular design also simplifies the task without requiring sophisticated algorithms to simulate the cardiac conduction system, since the model focuses on the input-output relationship of each module and the modular interactions instead. As summarized in Table 1 and described in details below, bi-directional interactions exist between 10 modular pairs: (1) RA conductor and AVJ, (2) RV conductor and AVJ, (3) ARG and RA conductor, (4) VRG and RV conductor, (5) RA lead and RA conductor, (6) RV lead and RV conductor, (7) RA lead and ARG, (8) RV lead and VRG, (9) pacemaker and RA lead, and (10) pacemaker and RV lead.

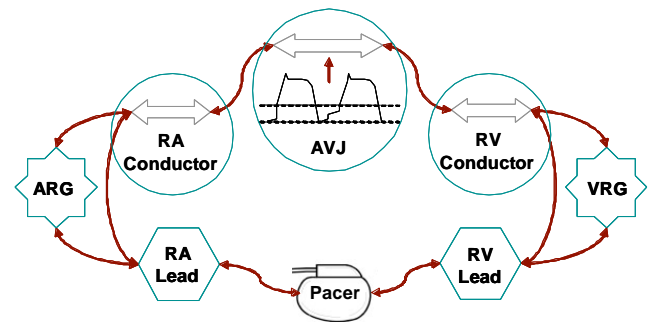


Fig. (2). Schematic diagram of the IDHP model structure. Modified from [15] with permission (© 2008, Biomedical Engineering Society).

Table 1. Bi-Directional Interactions Between IDHP Modules

Module A	Module B	A → B	B → A
RA conductor	AVJ	An antegrade wave in RA conductor invades the AVJ.	An escaping wave from AVJ starts retrograde conduction in the RA conductor.
RV conductor	AVJ	A retrograde wave in RV conductor invades the AVJ.	An escaping wave from AVJ starts antegrade conduction in the RV conductor.
ARG	RA conductor	An ARG impulse output starts an antegrade wave in the RA conductor.	A retrograde wave in the RA conductor resets the ARG.
VRG	RV conductor	A VRG impulse output starts a retrograde wave in the RV conductor.	An antegrade wave in the RV conductor resets the VRG.
RA lead	RA conductor	A captured AP from RA lead starts an antegrade wave in the RA conductor.	The RA lead senses the retrograde wave in the RA conductor.
RV lead	RV conductor	A captured VP from RV lead starts a retrograde wave in the RV conductor.	The RV lead senses the antegrade wave in the RV conductor.
RA lead	ARG	A supra-threshold AP from the RA lead resets the ARG.	The RA lead senses the ARG output.
RV lead	VRG	A supra-threshold VP from the RV lead resets the VRG.	The RV lead senses the VRG output.
Pacer	RA lead	Pacer delivers AP through RA lead.	Pacer analyzes the signal sensed by the RA lead.
Pacer	RV lead	Pacer delivers VP through RV lead.	Pacer analyzes the signal sensed by the RV lead.

A. Atrial Rhythm Generator

By changing impulse strength and arrival interval, the ARG module currently supports generating 5 types of atrial rhythms:

- Normal sinus rhythm with fixed atrial intervals, or random atrial intervals with predefined probability distribution (Gaussian or uniform). Each ARG output impulse usually has sufficient strength to depolarize the AVJ.
- AF rhythm with Poisson distribution of impulse arrival rate (note: arrival intervals follow truncated exponential distribution [11]). The strength of ARG output impulse usually varies randomly according to predefined Gaussian distribution.
- Atrial ectopic rhythm with predefined incidence rate (probability per cycle defined by uniform distribution) and predefined range of atrial coupling interval (defined by uniform distribution). Each ectopic beat has sufficient strength to depolarize the AVJ.
- Simulated atrial pacing protocol with programmed S1-S2 or S1-S2-S3 sequences, where S1 represents a train of atrial stimuli with fixed cycle length, and S2 and S3 represent premature stimuli with various coupling intervals [14, 19, 20]. Each atrial stimulation pulse has sufficient strength to depolarize the AVJ.
- Custom rhythm supported by importing atrial intervals from external files representing user-selected atrial rhythms (e.g., atrial intervals with predefined HRV). Each ARG output impulse has sufficient strength to depolarize the AVJ.

The ARG has bidirectional connections with two other modules: RA conductor and RA lead. An ARG impulse output can initiate an antegrade wave (toward AVJ) in the RA conductor. Meanwhile, it feeds input to the RA lead for atrial sensing (AS). On the other hand, the ARG is reset by either a retrograde wave (escaping from AVJ) in the RA conductor, or a supra-threshold atrial pace (AP) delivered by the RA lead.

In addition, the ARG module can also generate exogenous atrial noise with predefined incidence rate (probability per sample defined by uniform distribution), which can be sensed by the RA lead, but cannot start activation wave in the RA conductor nor reset the ARG.

B. Ventricular Rhythm Generator

As the counterpart of ARG, the VRG module can produce limited (two) types of intrinsic ventricular rhythms:

- Ventricular escape rhythm with fixed ventricular intervals, or random ventricular intervals with predefined probability distribution (Gaussian, uniform, or exponential), which are usually long to simulate slow escape rate, but can be short to simulate ventricular tachyarrhythmia.
- Ventricular ectopic rhythm with predefined incidence rate (probability per cycle defined by uniform

distribution) and predefined range of ventricular coupling interval (defined by uniform distribution).

The VRG has bidirectional connections with RV conductor and RV lead modules. An impulse output from the VRG can initiate a retrograde wave (toward AVJ) in the RV conductor. Meanwhile, it feeds the input of RV lead for ventricular sensing (VS). On the other hand, the VRG is reset by either an antegrade wave (escaping from AVJ) in the RV conductor, or a supra-threshold VP delivered by the RV lead.

Similarly, the VRG module can also generate exogenous ventricular noise with predefined incidence rate (probability per sample defined by uniform distribution), which can be sensed by the RV lead, but cannot generate activation wave in the RV conductor nor reset the VRG.

C. Right Atrial Conductor

Connecting AVJ on one end, and interfacing with ARG and RA lead on the other end, the RA conductor supports bi-directional atrial conductions. The antegrade atrial conduction is started by either an ARG impulse output or a captured AP, and is terminated when the antegrade wave invades the AVJ, or fuses with a retrograde conducted wave. Conversely, the retrograde atrial conduction is started after the completion of a retrograde AV conduction (escaping from AVJ), and is terminated when the retrograde wave reaches the ARG or fuses with an antegrade conducted wave.

The RA conductor is characterized by three programmable parameters: the antegrade atrial conduction time, the retrograde atrial conduction time, and the atrial refractory period. An atrial activation wave (antegrade or retrograde) cannot be started unless the RA conductor completes the atrial refractory period since its last activation.

D. Right Ventricular Conductor

As the counterpart of RA conductor, the RV conductor links AVJ with VRG and RV lead to support bi-directional ventricular conductions. The retrograde ventricular conduction is started by either a VRG output or a captured VP, and is terminated when the retrograde wave reaches the AVJ or fuses with an antegrade conducted wave. Conversely, an antegrade ventricular conduction is started after the completion of an antegrade AV conduction (escaping from AVJ), and is terminated when the antegrade wave conducts to the VRG, or fuses with a retrograde conducted wave.

Likewise, the RV conductor is characterized by three programmable parameters: the antegrade ventricular conduction time, the retrograde ventricular conduction time, and the ventricular refractory period. A ventricular activation wave (antegrade or retrograde) cannot be started when the RV conductor is still in ventricular refractory period since its last activation.

E. AV Junction

As a relay unit between RA and RV, the AVJ is modeled as a lumped structure with defined automaticity, conductivity, and refractoriness [4, 11]. As illustrated in Fig.

3, the AVJ is excited (phase 0) when its membrane potential crosses the depolarization threshold. Then AVJ repolarizes (phases 1–3) and returns to the resting potential (phase 4). The refractory period (when no new excitation can occur) begins with phase 0 and extends into phase 3. During phase 4, the AVJ membrane potential rises linearly, and step increases after each invading antegrade/retrograde wave.

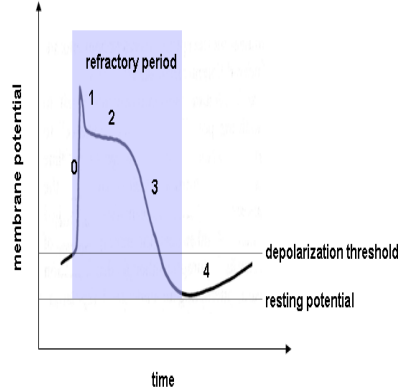


Fig. (3). Illustration of the depolarization and repolarization phases of the AVJ.

The excitation of AVJ generates an activation wave that starts an antegrade or retrograde AV conduction. If AVJ is antegrade excited while a retrograde wave is still active or vice versa, both activation waves are annihilated due to fusion. Otherwise, the antegrade or retrograde wave exits the AVJ upon its completion and invades RV or RA, respectively. Both AVJ conduction delay and refractory period are functions of its recovery time (T_{REC}), which is the time elapsed since the end of last AVJ refractory period. Specifically, the AV conduction delay (AVD) is modeled as [6, 9-11]

$$AVD = AVD_{min} + \alpha \exp(-T_{REC} / \tau_c) \quad (1)$$

where AVD_{min} is the shortest AVD when $T_{REC} \rightarrow \infty$, α is the longest extension of AVD when $T_{REC} = 0$, and τ_c is the conduction time constant. The AVJ refractory period (τ) is modeled as [4, 11]

$$\tau = \tau_{min} + \beta(1 - \exp(-T_{REC} / \tau_r)) \quad (2)$$

where τ_{min} is the shortest τ when $T_{REC} = 0$, β is the longest extension of τ when $T_{REC} \rightarrow \infty$, and τ_r is the refractory time constant. In addition, the electrotonic modulation is simulated by assuming τ is prolonged by a concealed impulse [6, 7, 11]

$$\Delta\tau = \tau_{min} (t / \tau_0)^\theta (\min(1, \Delta V / (V_T - V_R)))^\delta \quad (3)$$

where τ_0 is the original AVJ refractory period, $\Delta\tau$ is the extension of τ , and t is the time of impulse blockage ($0 < t < \tau_0$). The degree of τ extension depends on both the timing and strength of the blocked impulse, which are respectively modulated by two positive parameters θ and δ .

F. Right Atrial Lead

Connecting the pacer with ARG and RA conductor, the RA lead supports both AP and AS. On one hand, the AP pulse is delivered through the RA lead. It captures the atrium

if the RA conductor is not refractory and the AP strength is greater than a predefined AP threshold. The captured AP resets the ARG, and starts an antegrade wave in the RA conductor. No effect follows a non-capture AP. On the other hand, the RA lead picks up electrical signals in the atrium, which could be intrinsic atrial depolarizations (including ARG output and retrograde atrial activation), or exogenous atrial noise (generated by the ARG module).

G. Right Ventricular Lead

Similarly, the RV lead connects the pacer with VRG and RV conductor. On one hand, the VP pulse is delivered *via* the RV lead. It captures the ventricle if the RV conductor is not refractory and the VP strength is greater than a predefined VP threshold. The captured VP resets the VRG, and starts a retrograde wave in the RV conductor. No effect follows a non-capture VP. On the other hand, the RV lead senses electrical signals in the ventricle, which could be intrinsic ventricular depolarizations (including VRG output and antegrade ventricular activation), or exogenous ventricular noise (generated by the VRG module).

H. Dual-Chamber Pacer

The dual-chamber pacer interacts with the heart through RA and RV leads. Specifically, the pacer module classifies atrial and ventricular senses, and controls the timing of AP and VP, according to various industry-standard pacing modes, such as DDD, DDI, VVI, AAI, etc [21]. As described in details in the next section, the pacer maintains a plural of timers and windows to perform sense event classification and pace timing control.

In addition, the pacer module provides support of continuous interval measurement, including but not limited to, the A-A intervals, the V-V intervals, the A-V intervals, the V-A intervals, etc., based on which the pacer can perform rate and rhythm analysis, log diagnostic statistics, and implement advanced pacing algorithms.

III. MODEL IMPLEMENTATION

Fig. 4 shows the top level diagram of IDHP model implementation.

First, the simulation reads model parameters from an external configuration file. The model parameters are divided into nine groups, corresponding to the simulation environment and eight modular components, respectively. An exemplary list of model parameters is shown in Table 2.

Then the simulation initializes model variables including various timers, flags, counters, etc. Table 3 lists main timers associated with the heart modules and their start and stop conditions. Major pacer timers and their associated pacer intervals/windows are summarized in Table 4. Note that the detailed pacer timing logic and the naming convention usually vary between different manufacturers, and may also vary for different pacer models from the same manufacturer. On the other hand, the pacer timers, intervals, and windows simulated in the IDHP model represent a generic form of pacer timing control that is fairly standard in most modern dual-chamber pacemakers.

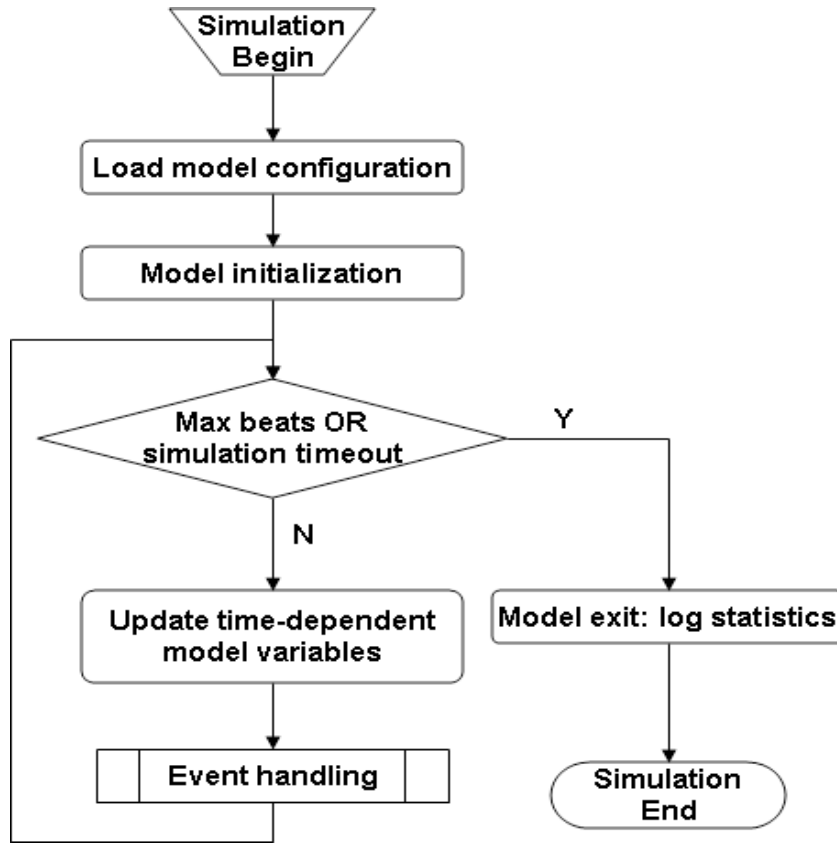


Fig. (4). Top-level flowchart of running IDHP model simulation. Modified from [15] with permission (© 2008, Biomedical Engineering Society).

Table 2. List of an Exemplary Set of Model Parameters

Parameter (unit)	Value	Comments
// Simulation environment parameters		
fnRR	= outrr1.txt	// output RR (V-V) interval filename
fnPP	= outpp1.txt	// output PP (A-A) interval filename
fnPR	= outpr1.txt	// output PR (A-V) interval and AVJ status filename
fnMK	= outmk1.txt	// output event marker filename
fnLOG	= outlog1.txt	// output event log filename
MAX_BEAT	= 10	// max ventricular beats to run
MAX_TIME(s)	= 100	// max simulation time to run
Ts(s)	= 0.001	// sampling interval
RR0(s)	= 1.0	// initial RR interval
// ARG module parameters		
ARG_MODEL	= 3	// 1-exp, 2-uni, 3-normal, 4-S1S2, 5-S1S2S3, 6-ext, others-fixed
lambda(1/s)	= 1	// mean arrival rate of ARG impulses (mean interval = 60/lambda)
AAstd(s)	= 0.05	// standard deviation of ARG output intervals
dVmean(mV)	= 50	// mean AVJ potential incr. (ΔV) by ARG impulse bombardment
dVstd(mV)	= 0	// standard deviation of ΔV
S1S2(s)	= 0.2	// S1S2 interval of atrial pacing protocol

Table 2. contd....

Parameter (unit)	Value	Comments
S2S3(s)	= 0.5	// S2S3 interval of atrial pacing protocol
AES_Prob	= 0.005	// probability of atrial extra-systole (per atrial cycle)
AES_CII	= 0.2	// shortest possible coupling interval of atrial extra-systole
AES_CT2	= 0.6	// longest possible coupling interval of atrial extra-systole
ANZ_Prob	= 1e-6	// probability of atrial noise (per sample)
// VRG module parameters		
VRG_MODEL	= 3	// 1-exponential, 2-uniform, 3-Gaussian, 4-external, others-fixed
VVmean(s)	= 3.0	// mean VRG output interval (mean escape rate = 60/VVmean)
VVstd(s)	= 0.05	// standard deviation of VRG output interval
VES_Prob	= 0.005	// probability of ventricular extra-systole (per ventricle cycle)
VES_CII	= 0.3	// shortest possible coupling interval of ventricular extra-systole
VES_CT2	= 0.6	// longest possible coupling interval of ventricular extra-systole
VNZ_Prob	= 1e-6	// probability of ventricular noise (per sample)
// RA conductor module parameters		
AtrAntDly(s)	= 0.03	// antegrade conduction delay from ARG to AVJ
AtrRetDly(s)	= 0.03	// retrograde conduction delay from AVJ to ARG
AtrRef(s)	= 0.05	// atrial refractory period
// RV conductor module parameters		
VtrAntDly(s)	= 0.05	// antegrade conduction delay from AVJ to VRG
VtrRetDly(s)	= 0.1	// retrograde conduction delay from VRG to AVJ
VtrRef(s)	= 0.2	// ventricular refractory period
// AVJ module parameters		
Vt(mV)	= -40	// AVJ depolarization threshold potential
Vr(mV)	= -90	// AVJ resting membrane potential
dVdt(mV/s)	= 30	// AVJ spontaneous depolarization slope
MinAVDa(s)	= 0.1	// shortest possible antegrade AV conduction time
MinAVDr(s)	= 0.1	// shortest possible retrograde AV conduction time
alpha(s)	= 0.15	// longest possible extension of AV conduction time
tau_c(s)	= 0.1	// time constant of AV conduction time vs. AVJ recovery time
MinRef(s)	= 0.05	// shortest possible AVJ refractory period
beta(s)	= 0.25	// longest possible extension of AVJ refractory period
tau_r(s)	= 0.5	// time constant of AVJ refractory period vs. AVJ recovery time
Ref_std(s)	= 0	// standard deviation of AVJ refractory period
delta	= 10	// concealed electrotonic modulation affected by impulse strength
theta	= 10	// concealed electrotonic modulation affected by impulse timing
// RA lead module parameters		
ApThresh(V)	= 1.0	// AP threshold
// RV lead module parameters		
VpThresh(V)	= 1.0	// VP threshold
// Pacer module parameters		
MODE	= DDD	// pacing mode: AOO, VOO, AAI, VVI, DVI, DDI, DDD
BI(s)	= 1.0	// standby pacing basic interval (a.k.a. lower rate limit)

Table 2. contd....

Parameter (unit)	Value	Comments
AVDp(s)	= 0.18	// paced AV delay (started after each AP in DDD mode)
AVDs(s)	= 0.16	// sensed AV delay (started after each AS in DDD mode)
PVARP(s)	= 0.325	// post-ventricular atrial refractory period (PVARP)
PVARPext(s)	= 0	// PVARP extension after ventricular extra-systole (DDD mode)
FFBp(s)	= 0.15	// far-field blanking window after VP
FFBs(s)	= 0.1	// far-field blanking window after VS
ARP(s)	= 0.3	// pacemaker atrial refractory period
VRP(s)	= 0.25	// pacemaker ventricular refractory period
PVAB(s)	= 0.035	// post-VP atrial blanking window (x-channel VP blanking)
PAVB(s)	= 0.07	// post-AP ventricular blanking window (x-channel AP blanking)
IPAB(s)	= 0.125	// post-AP atrial blanking window (in-channel AP blanking)
IPVB(s)	= 0.11	// post-VP ventricular blanking window (in-channel VP blanking)
ISAB(s)	= 0.125	// post-AS atrial blanking window (in-channel AS blanking)
ISVB(s)	= 0.1	// post-VS ventricular blanking window (in-channel VS blanking)
UTI(s)	= 0.5	// upper tracking interval (upper tracking rate = 60/UTI)
SW(s)	= 0.1	// safety window
AP_AMP(V)	= 3.6	// AP amplitude
VP_AMP(V)	= 3.6	// VP amplitude
VRS_METHOD	= 0	// reserved for other pacing algorithms

Table 3. List of Major Timers Associated with the Heart Modules of the IDHP Model

Timer	Start Condition	Stop Condition
<i>arg.t</i> (ARG timer)	ARG output, or ARG reset by AP or retrograde atrial conduction	Next ARG output, or ARG reset by AP or retrograde atrial conduction
<i>vrg.t</i> (VRG timer)	VRG output, or VRG reset by VP or antegrade ventricular conduction	Next VRG output, or VRG reset by VP or antegrade ventricular conduction
<i>avj.t</i> (AVJ refractory timer)	Start of AVJ refractory period caused by AVJ activation	End of AVJ refractory period
<i>avj.tA</i> (Antegrade AVJ timer)	Antegrade AVJ activation	Completion of antegrade AV conduction, or fusion with a retrograde AV conduction
<i>avj.tR</i> (Retrograde AVJ timer)	Retrograde AVJ activation	Completion of retrograde AV conduction, or fusion with an antegrade AV conduction
<i>atr.tA</i> (Antegrade atrial timer)	Start of antegrade atrial conduction caused by ARG output or captured AP	Completion of antegrade atrial conduction, or fusion with a retrograde atrial conduction
<i>atr.tR</i> (Retrograde atrial timer)	Start of retrograde atrial conduction when a retrograde wave exits the AVJ	Completion of retrograde atrial conduction, or fusion with an antegrade atrial conduction
<i>vtr.tA</i> (Antegrade ventricle timer)	Start of antegrade ventricular conduction when an antegrade wave exits the AVJ	Completion of antegrade ventricular conduction, or fusion with a retrograde ventricular conduction
<i>vtr.tR</i> (Retrograde ventricle timer)	Start of retrograde ventricular conduction caused by VRG output or captured VP	Completion of retrograde ventricular conduction, or fusion with an antegrade ventricular conduction

Table 4. List of Major Timers Associated with the Pacer Module of the IDHP Model

Timer	Related Pacer Intervals/Windows	Brief Description
tAP (AP timer)	Basic interval, AV delay	Start and stop conditions depend on pacing mode (atrial or ventricle based timing). Timeout of tAP triggers an AP.
tVP (VP timer)	Basic interval, AV delay, safety window	Start and stop conditions depend on pacing mode (atrial or ventricle based timing). Timeout of tVP triggers a VP.
$tAVD$ (AV delay timer)	AV delay	In DDD mode, VS detected in AV delay inhibits VP. In DDI mode, VA delay equals the basic interval minus AV delay.
tSW (SW timer)	Safety window (SW)	In DDD mode, an AP starts a SW. If VS is detected in SW, VP will be delivered at the end of SW to prevent ventricular asystole.
tAB (ABW timer)	Atrial blanking window (ABW)	AP or AS starts in-channel ABW, and VP or VS starts cross-channel ABW. Any AS detected in ABW is ignored by the pacer.
tVB (VBW timer)	Ventricle blanking window (VBW)	VP or VS starts in-channel VBW, and AP or AS starts cross-channel VBW. Any VS detected in VBW is ignored by the pacer.
$tarp$ (ARP timer)	Atrial refractory period (ARP)	AS detected in ARP is considered refractory AS, which is usually ignored by the pacer (but may be used for advanced analysis).
$tVRP$ (VRP timer)	Ventricle refractory period (VRP)	VS detected in VRP is considered refractory VS, which is usually ignored by the pacer (but may be used for advanced analysis).
$tFFP$ (FFPW timer)	Far-field protection window (FFPW)	AS detected in FFPW is considered far-field senses of VP or VS, and is usually ignored by the pacer (but may be used for advanced analysis).
$tPVARP$ (PVARP timer)	Post-ventricular refractory period (PVARP)	AS detected in PVARP can be used for interval/rhythm analysis and timing control, e.g., to prevent pacemaker-mediated tachycardia in DDD mode.
$tUTI$ (UTI timer)	Upper tracking interval (UTI)	In DDD mode, UTI is applied after each VP, and sets the upper limit to the ventricular pacing rate.

The simulation runs at the predefined sampling frequency. At each sample time, the model updates its time-dependent variables (e.g., AVJ membrane potential, active timers), and then handles possible event(s). The simulation continues until a predefined number of cardiac beats are generated or the simulation time runs out, when the model logs statistics and exits.

The overall event handling routine is illustrated in Fig. 5, where the AP/AS handling and VP/VS handling are further described in Fig. 6. The simulation checks model timers and status flags to detect various events and calls for respective functions as necessary. For example, atrial or ventricular fusion (*AtrFusion* or *VtrFusion*) occurs when antegrade and retrograde waves collide in the RA or RV, respectively. Completion of antegrade RA or retrograde RV conduction leads to antegrade or retrograde invasion of AVJ (*AnteHitAvj* or *RetrHitAvj*), and the wave escapes from the AVJ (*AnteEscAvj* or *RetrEscAvj*) upon finishing antegrade or retrograde AV conduction. The AVJ is activated (*ActivateAvj*) and becomes refractory (*StartAvjRef*) if its membrane potential crosses the depolarization threshold, whereas the end of AVJ refractory period starts the phase 4 (*StartAvjPh4*). Pacer delivers AP or VP (*AtrPace* or *VtrPace*) based on programmed timing logic. Atrial sense (*AtrSense*) is caused by ARG output (*ArgOutput*), retrograde RA activation, or atrial noise, and ventricle sense (*VtrSense*) is caused by VRG output (*VrgOutput*), antegrade RV activation, or ventricle noise. Table 5 summarizes the major events simulated in the IDHP model, their occurrence conditions, and the respective service actions to be taken (see [15] for detailed function flowcharts).

As emphasized above, different pacer models usually differ in their control algorithms related to pacing and sensing (*AtrPace*, *VtrPace*, *AtrSense*, *VtrSense*). Moreover, the timing control logics of pacers also vary between different pacing modes (Fig. 7). For instance, the standard DDD mode is an atrial-tracking mode, that is, pacer's basic interval and AV delay start with each AP or AS. Timeout of the basic interval triggers an AP, and timeout of the AV delay triggers a VP. An AS event detected during the basic interval inhibits the AP, and a VS event detected during the AV delay inhibits the VP. In addition, a pacer-classified ventricular extra-systole (VES) reschedules the next AP at the calculated VA delay. Contrarily, the standard DDI mode is a non-atrial tracking mode. The pacer's basic interval and VA delay starts with each VP or VS. Timeout of the basic interval triggers a VP, and timeout of the VA delay triggers an AP. A VS event detected during the basic interval inhibits the VP, and an AS event detected during the VA delay inhibits the AP.

IV. MODEL APPLICATIONS

In this section, some representative, albeit not exhaustive, examples are given to demonstrate how to use the IDHP model to simulate various intrinsic heart rhythms and their interactions with standard dual-chamber cardiac pacing and sensing (Figs. 8-15), by simply editing model parameters in the configuration file (Table 6). Optionally, a random seed number can be specified at model run time for repeatability. Additional examples of incorporating more advanced pacing algorithms into the IDHP model are also presented (Figs. 16-18).

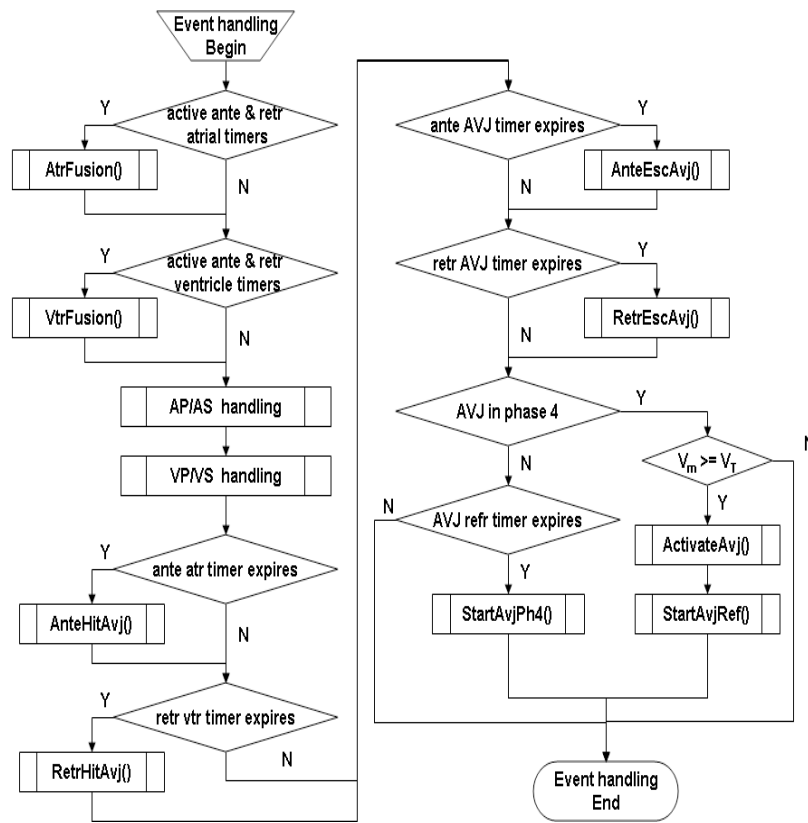


Fig. (5). General event handling routines implemented in IDHP model. Modified from [15] with permission (© 2008, Biomedical Engineering Society).

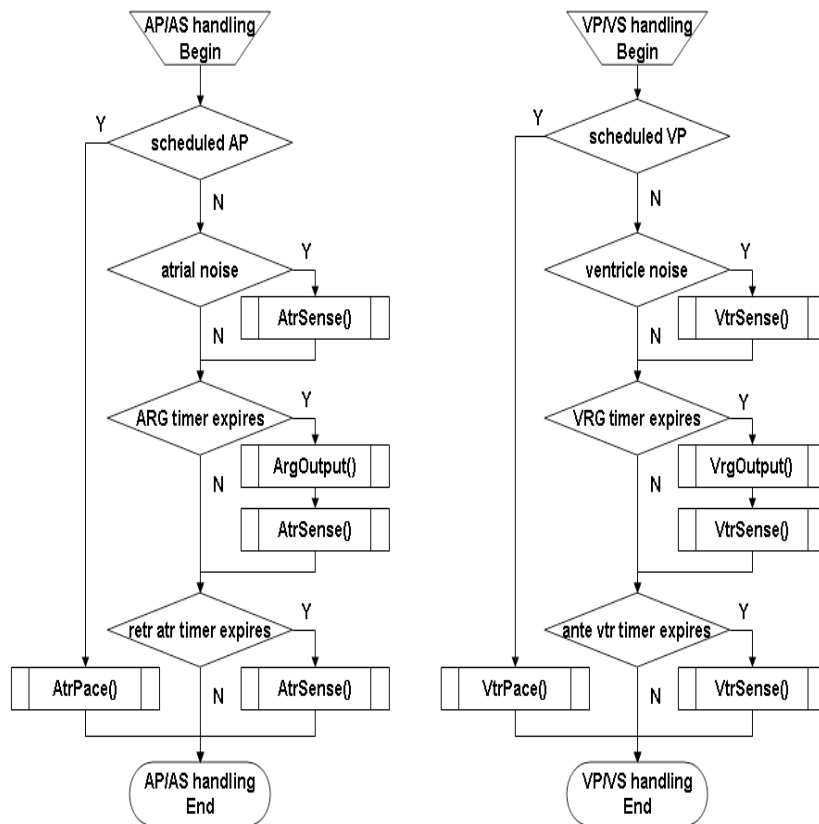


Fig. (6). Event handling routines implemented in IDHP model for AP/AS events (left) and VP/VS events (right). Modified from [15] with permission (© 2008, Biomedical Engineering Society).

Table 5. Summary of Major Events Handled by the IDHP Model

Function (Event)	Condition	Actions
<i>AtrFusion</i> (Atrial fusion)	Both antegrade and retrograde atrial timers are active	Stop both antegrade and retrograde atrial timers.
<i>VtrFusion</i> (Ventricle fusion)	Both antegrade and retrograde ventricle timers are active	Stop both antegrade and retrograde ventricle timers.
<i>ArgOutput</i> (ARG output)	ARG timer expires (end of the atrial interval)	Get atrial impulse strength. Start a new ARG timer (get next atrial interval). Start an antegrade atrial timer if atrium is non-refractory.
<i>VrgOutput</i> (VRG output)	VRG timer expires (end of the ventricle interval)	Get ventricle impulse strength. Start a new VRG timer (get next ventricle interval). Start a retrograde ventricle timer if ventricle is non-refractory.
<i>AnteHitAvj</i> (Antegrade AVJ invasion)	Antegrade atrial timer expires	If AVJ is in phase 4, then increment its membrane potential based on atrial impulse strength. If AVJ is refractory, then modulate the AVJ refractory period, and stop the retrograde AVJ timer if any.
<i>RetrHitAvj</i> (Retrograde AVJ invasion)	Retrograde ventricle timer expires	If AVJ is in phase 4, then increment its membrane potential based on ventricle impulse strength. If AVJ is refractory, then modulate the AVJ refractory period, and stop the antegrade AVJ timer if any.
<i>AnteEscAvj</i> (Antegrade escape of AVJ)	Antegrade AVJ timer expires	Start an antegrade ventricle timer.
<i>RetrEscAvj</i> (Retrograde escape of AVJ)	Retrograde AVJ timer expires	Start a retrograde atrial timer.
<i>ActivateAvj</i> (Activation of AVJ)	AVJ is in phase 4 and its membrane potential crosses the depolarization threshold	Calculate AV conduction time. For antegrade activation, start an antegrade AVJ timer if there is no active retrograde AVJ timer; otherwise, stop the retrograde AVJ timer. For retrograde activation, start a retrograde AVJ timer if there is no active antegrade AVJ timer; otherwise, stop the antegrade AVJ timer.
<i>StartAvjRef</i> (Start of AVJ refractory)	AVJ is in phase 4 and its membrane potential crosses the depolarization threshold	Calculate AVJ refractory period and start the AVJ refractory timer.
<i>StartAvjPh4</i> (Start of AVJ phase 4)	AVJ refractory timer expires	Reset AVJ membrane potential to the resting potential.
<i>AtrPace</i> (Delivery of atrial pace)	AP timer expires	If AP amplitude is supra-threshold and atrium is non-refractory, then start an antegrade atrial timer, and restart the ARG timer (ARG reset). Update pacer timers (pacer model and mode specific). Update pacer measured intervals (e.g., V-A, A-A, etc.). Update pacer statistics and log event markers.
<i>VtrPace</i> (Delivery of ventricle pace)	VP timer expires	If VP amplitude is supra-threshold ventricle is non-refractory, then start a retrograde ventricle timer, and restart the VRG timer (VRG reset). Update pacer timers (pacer model and mode specific). Update pacer measured intervals (e.g., V-V, A-V, etc.). Update pacer statistics and log event markers.
<i>AtrSense</i> (Atrial sense detection)	Atrial noise occurs, or ARG timer expires, or retrograde atrial timer expires	If retrograde atrial timer expires, then restart the ARG timer (ARG reset). Classify AS event type (pacer model and mode specific) Update pacer timers (pacer model and mode specific). Update pacer measured intervals (e.g., V-A, A-A, etc.). Update pacer statistics and log event markers.
<i>VtrSense</i> (Ventricle sense detection)	Ventricle noise occurs, or VRG timer expires, or antegrade ventricle timer expires	If antegrade ventricle timer expires, then restart the VRG timer (VRG reset). Classify VS event type (pacer model and mode specific) Update pacer timers (pacer model and mode specific). Update pacer measured intervals (e.g., V-V, A-V, etc.). Update pacer statistics and log event markers.

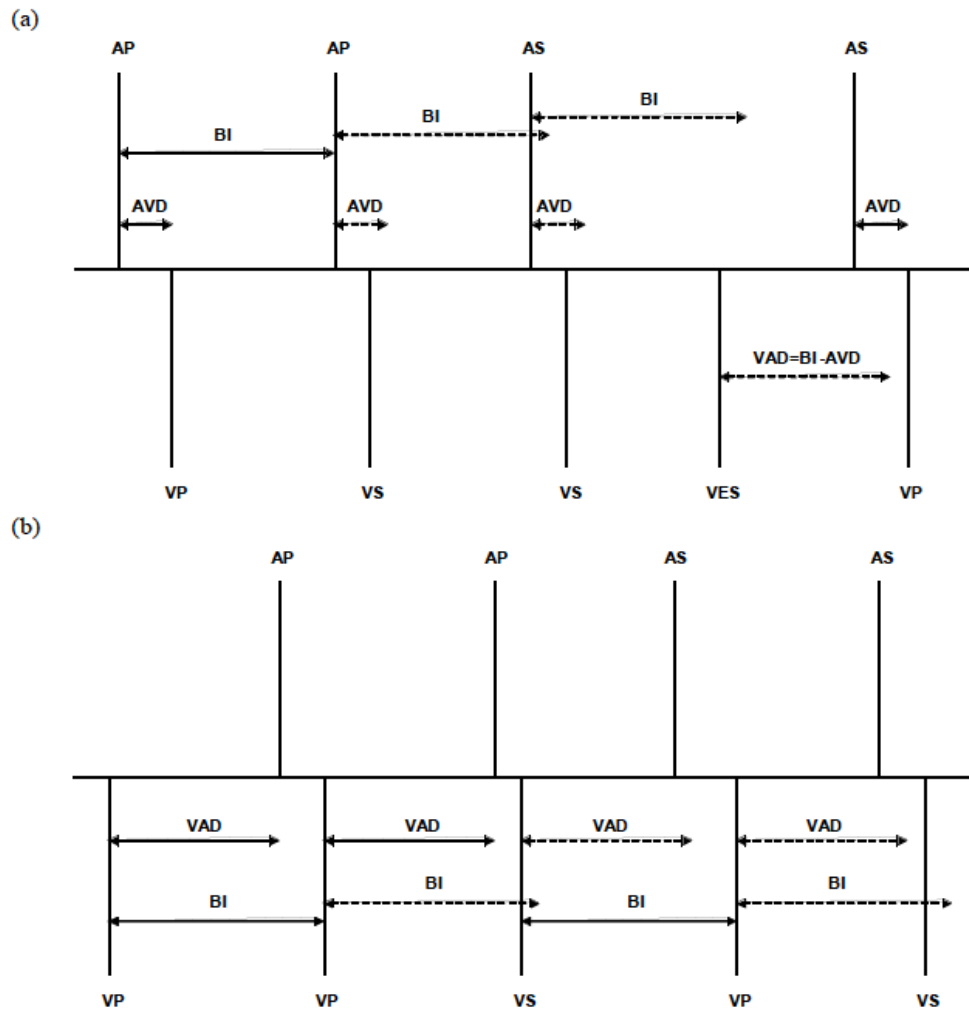


Fig. (7). Schematic illustration of the pacemaker timing in (a) DDD mode and (b) DDI mode. BI: basic interval; AVD: AV delay; VAD: VA delay; VES: ventricular extra-systole. Reprinted from [15] with permission (© 2008, Biomedical Engineering Society).

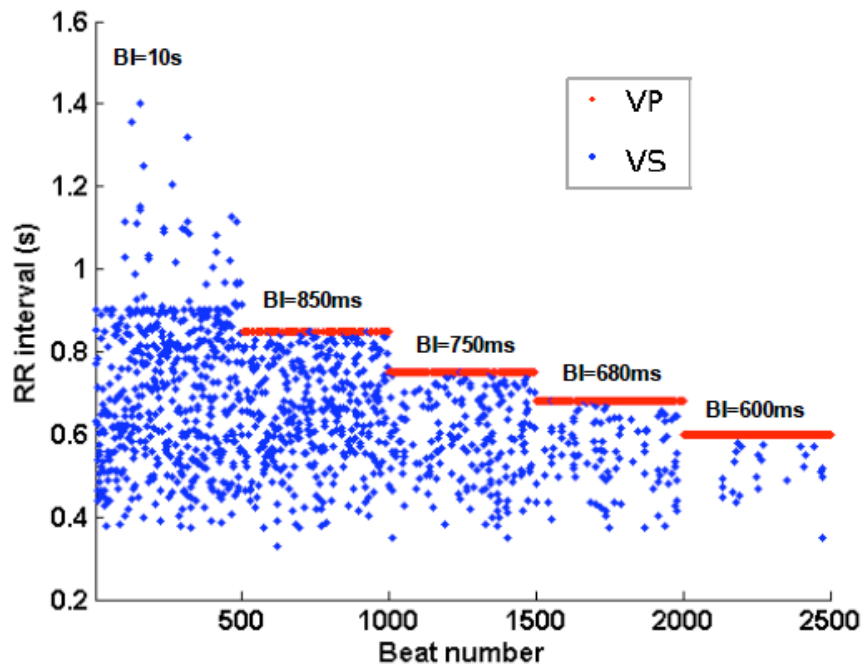


Fig. (8). Model simulated RR intervals during AF while the pacer operates in VVI mode with varying basic intervals.

Table 6. List of Model Parameter Changes from Table 2 to Produce Fig. 8-Fig. 15.

Parameter	Value	Comments
// Parameter changes to produce Fig. 8. (random seed = 1)		
MAX_BEAT	= 500	// 500 ventricular beats for each BI
ARG_MODEL	= 1	// exponential distribution of AF intervals (arrival rate: Poisson)
lambda(1/s)	= 5	// mean arrival rate of AF impulses
dVmean(mV)	= 15	// mean AVJ potential increment by AF bombardment
MODE	= VVI	// VVI (non-atrial tracking) mode
BI (s)	= 10	// basic interval, also run with BI = 0.85, 0.75, 0.68, 0.60
// Parameter changes to produce Fig. 9. (random seed = 1)		
AES_Prob	= 0.1	// increase probability of atrial extra-systole
VES_Prob	= 0.1	// increase probability of ventricular extra-systole
AVDp(s)	= 0.20	// paced AV delay
AVDs(s)	= 0.18	// sensed AV delay
// Parameter changes to produce Fig. 10. (random seed = 5)		
AP_AMP(V)	= 0.8	// sub-threshold AP threshold
// Parameter changes to produce Fig. 11. (random seed = 11)		
ANZ_Prob	= 5e-4	// increase probability of atrial noise
VNZ_Prob	= 5e-4	// increase probability of ventricular noise
// Parameter changes to produce Fig. 12. (random seed = 8)		
lambda(1/s)	= 2.1	// atrial rate (about 126 beats/min)
MinAVDa(s)	= 0.5	// antegrade AV block (pacemaker dependent)
MinAVDr(s)	= 0.5	// retrograde AV block (no retrograde AS)
AVDp(s)	= 0.12	// shorten AV delay after AP
AVDs(s)	= 0.12	// shorten AV delay after AS
// Parameter changes to produce Fig. 13. (random seed = 4)		
VES_Prob	= 0.1	// increase probability of ventricular extra-systole
PVARP(s)	= 0.2	// shorten post-ventricular atrial refractory period
// Parameter changes to produce Fig. 14. (random seed = 1)		
lambda(1/s)	= 3	// high atrial rate (180 beats/min)
MinAVDa(s)	= 0.5	// antegrade AV block (pacemaker dependent)
MinAVDr(s)	= 0.5	// retrograde AV block (no retrograde AS)
// Parameter changes to produce Fig. 15. (random seed = 6)		
ARG_MODEL	= 1	// exponential distribution of AF intervals (arrival rate: Poisson)
lambda(1/s)	= 3	// mean arrival rate of AF impulses
dVmean(mV)	= 30	// mean AVJ potential increment by AF bombardment
MODE	= DDI	// DDI (non-atrial tracking) mode
BI (s)	= 0.75	// basic interval during mode switch

In the first example, Fig. 8 shows the model-generated RR intervals during AF while the pacemaker operates in VVI mode. Five separate sequences of 500 RR intervals are generated by varying the pacemaker's basic interval (BI). The ventricular response during intrinsic AF (BI = 10s, no VP) is characterized by short and irregular RR intervals. Progressively shortening the BI (850ms, 750ms, 680ms, 600ms) leads to higher percentage of VP (respectively 28.8%, 59.6%, 75.6%, 92%) and increased stabilization of the ventricular rate. Consistent with previous findings [12], VP not only eliminates long ventricular pauses, but also suppresses short intrinsic RR intervals in AF.

In the following examples (Figs. 9-18), each figure shows a segment of the model generated event markers. In these figures, sense and pace events are marked by vertical lines: atrial events shown in the upper plot and ventricular events shown in the lower plot. Each event has a symbol indicating pacemaker-classified event type: pace (circle); sense (triangle); VES (pentagram); refractory or far-field sense (star); undetected due to blanking (cross). Pace amplitudes (unit: V) are shown next to the pace markers. In addition, the following annotations are added to show the true event type: I – intrinsic depolarization; E – ectopic depolarization; N – noise; R – retrograde atrial depolarization; S – antegrade ventricular depolarization; C – captured pace; L – loss-of-capture pace.

Fig. 9 shows a segment of model generated event markers when the heart is in normal sinus rhythm and the pacemaker operates in DDD mode. The intrinsic sinus rate is similar to pacemaker's basic rate, and the intrinsic AV conduction time is comparable to programmed AV delay of the pacemaker. Thus both atrial and ventricular rhythms are mixed between paces and senses. In addition, a ventricular ectopic beat (classified as VES by the pacemaker) causes a retrograde AS, and an atrial ectopic beat causes an antegrade VS (but misclassified as VES by the pacemaker).

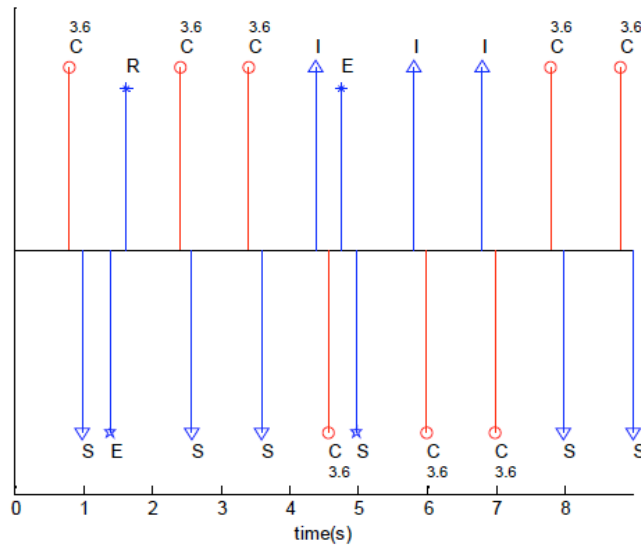


Fig. (9). An exemplary segment of model-generated event markers when the heart is in normal sinus rhythm with incidental atrial and ventricular ectopic beats, and the pacemaker operates in DDD mode.

Fig. 10 shows another segment of model generated event markers when the heart has normal sinus rhythm and the

pacemaker operates in DDD mode, but the AP amplitude (0.8V) is below the atrial threshold (1.0V). Since AP does not capture the atrium, the sinus rhythm is preserved, evidenced by either intrinsic atrial depolarization after AP (undetected by the pacemaker due to blanking, or detected as a far-field or refractory sense), or retrograde atrial depolarization after VP.

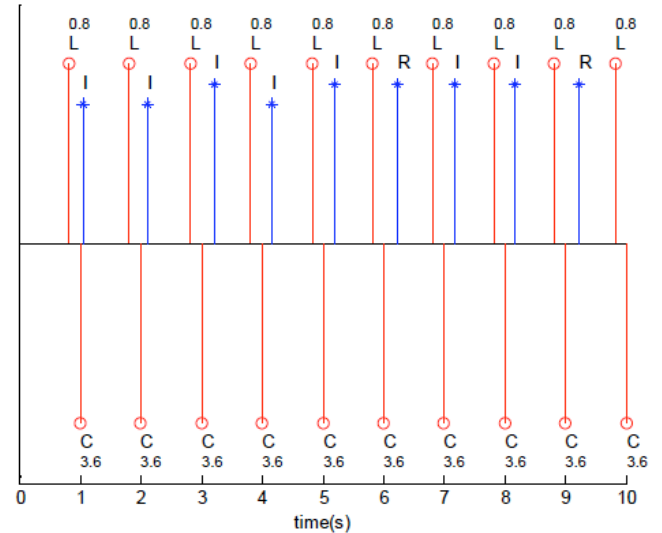


Fig. (10). An exemplary segment of model-generated event markers when the heart is in normal sinus rhythm, and the pacemaker operates in DDD mode but with sub-threshold AP amplitude.

Fig. 11 shows another simulated marker strip where the heart is in normal sinus rhythm and the pacemaker operates in DDD mode, but in the presence of exogenous noise. As expected, the noise events do not affect intrinsic rhythm, e.g., intrinsic AS occur shortly after noise AS (no ARG reset); but noise senses can affect pacemaker timing, e.g., noise AS are tracked to schedule VP, and noise VS classified as VES reschedule the following AP.

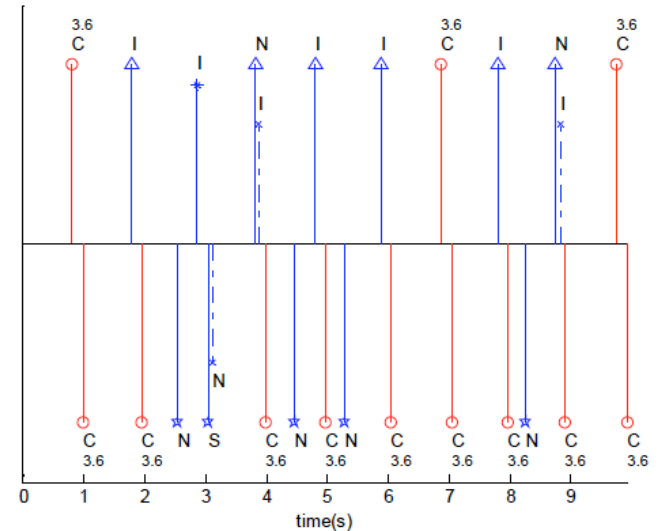


Fig. (11). An exemplary segment of model-generated event markers when the heart is in normal sinus rhythm and the pacemaker operates in DDD mode, but in the presence of exogenous noise.

Fig. 12 shows an example of simulated atrial tachycardia rhythm while the pacemaker operates in DDD mode, and the sinus

rate is slightly higher than the pacer's upper tracking rate. Each normal AS is tracked by the pacer and followed by a VP, which can only be delivered at the end of upper tracking interval (rather than the end of AV delay). This causes progressive lengthening of the AS-VP interval, until an AS falls in the post-ventricular atrial refractory period (PVARP), in which case no VP follows (i.e., periodic AV block). This is the well-known pacemaker Wenckebach behavior [21].

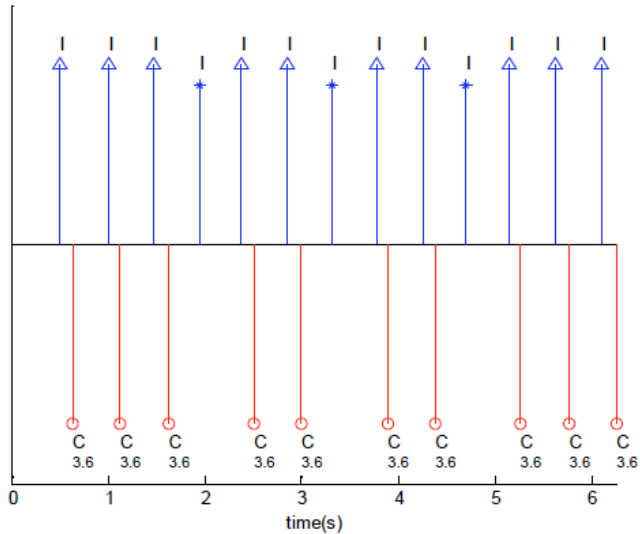


Fig. (12). An exemplary segment of model-generated event markers when the heart is in atrial tachycardia rhythm, and the pacer operates in DDD mode but the VP rate is limited by the programmed upper tracking rate.

Fig. 13 shows a typical example of simulated pacemaker-mediated tachycardia (PMT) episode [21]. The model configuration is similar to that of Fig. 9 except that the pacer's PVARP is shortened. After two cycles of baseline AP-VP rhythm in DDD mode, a ventricular ectopic beat causes retrograde atrial depolarization that is sensed outside the PVARP. The pacer tracked this detected AS by delivering a VP at the programmed AV delay. The VP causes another retrograde AS, and the sequence repeats, leading to an endless loop tachycardia.

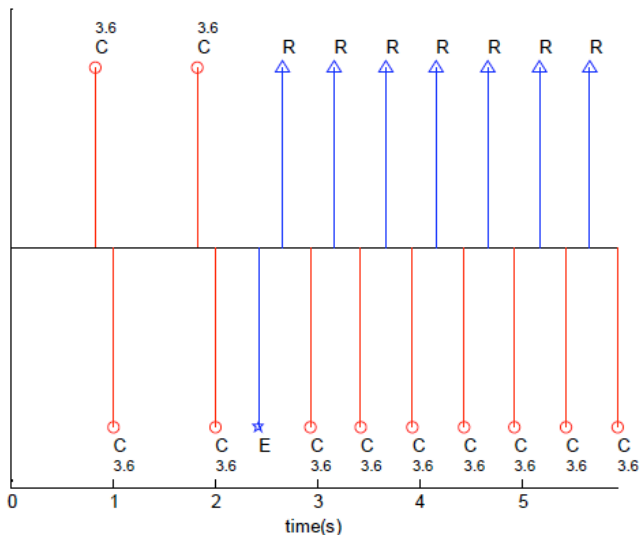


Fig. (13). An exemplary segment of model-generated event markers representing pacemaker-mediated tachycardia in DDD mode.

Fig. 14 shows another well-known pacemaker 'misbehavior' simulated by the model – 2:1 lock-in. In this case, the pacer fails to mode switch (from atrial-tracking DDD mode to non-atrial tracking DDI mode) at fast but stable atrial rate, because alternate atrial event falls either in the far-field blanking window or PVARP window. As a result, pacer fails to detect high atrial rate unless specific algorithm is applied to analyze the heart rhythm and break the 2:1 lock-in by dynamically adjusting pacer parameters [22].

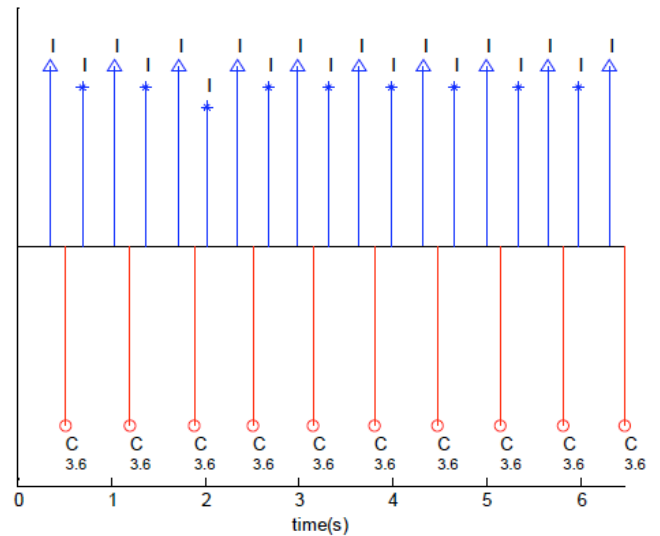


Fig. (14). An exemplary segment of model-generated event markers representing 2:1 lock-in during atrial tachycardia in DDD mode.

Fig. 15 shows a segment of simulated event markers when the heart is in AF rhythm and the pacer operates in DDI mode (as during mode switch). The fast and random arrival of AF impulses leads to short and irregular RR intervals (592 ± 134 ms). Evidently, some AF impulses are blocked and not conducted to the ventricle. Also note that one AP and two VPs fail to capture although they have

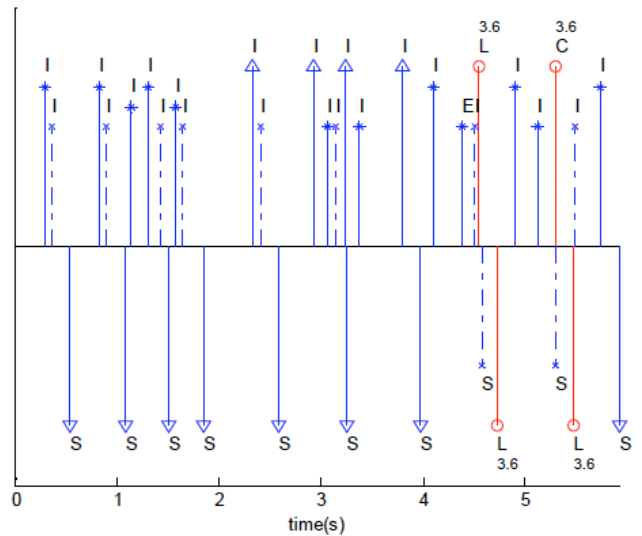


Fig. (15). An exemplary segment of model-generated event markers when the heart is in AF rhythm, and the pacer operates in DDI mode without ventricular rate smoothing.

supra-threshold (threshold 1.0V) pacing amplitude (3.6V). As shown in the figure, each of the non-capture AP or VP is immediately preceded by an intrinsic atrial or ventricular depolarization (but undetected by the pacer due to blanking) that renders the atrium or ventricle refractory.

Fig. 16 shows another episode of AF rhythm while the pacer operates in DDI mode. The model configuration is identical to that of Fig. 15 except that an adaptive ventricular rate smoothing (VRS) algorithm is incorporated into the model [12, 23]. By dynamically adjusting the VP rate based on previous RR intervals, the adaptive-VRS algorithm greatly improves the stability without significant shortening of the RR intervals ($570 \pm 77\text{ms}$).

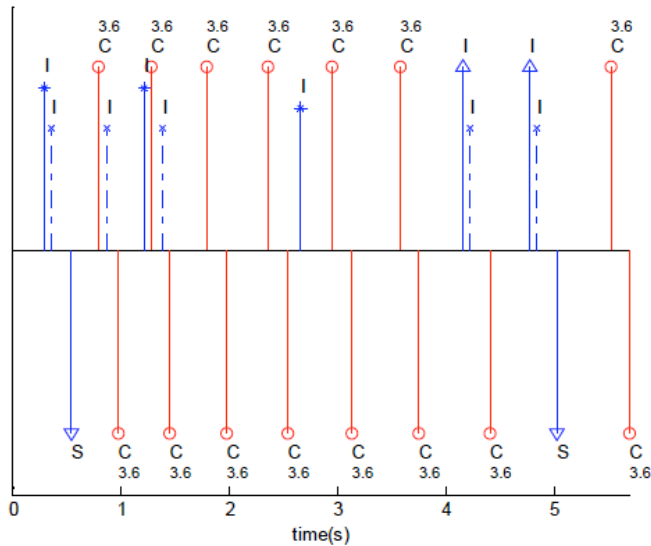


Fig. (16). An exemplary segment of model-generated event markers when the heart is in AF rhythm, and the pacer operates in DDI mode with adaptive-VRS algorithm.

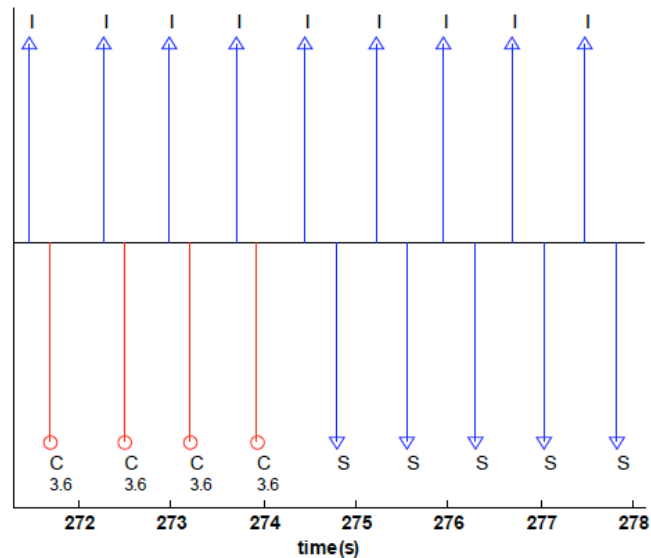


Fig. (17). An exemplary segment of model-generated event markers for applying scan AV hysteresis in the presence of first degree AV block. Reprinted from [24] with permission (© 2009, IEEE).

Fig. 17 and Fig. 18 illustrate two other examples by incorporating advanced pacing algorithm – AV hysteresis – into the IDHP model [24]. Fig. 17 shows an example of applying scan AV hysteresis in the presence of first degree AV block [24]. After delivering 180 consecutive VPs (only the last 4 VPs are shown in the figure), the pacer starts a scan AV hysteresis to search for intrinsic AV conduction by temporarily extending the pacer’s AV delay (for up to 5 cycles). Since VS is uncovered in the first cycle, the long AV delay is retained to promote VS and reduce VP.

Finally, Fig. 18 shows an example of applying repetitive AV hysteresis to encourage intrinsic AV conduction to return quickly during intermittent AV block [24]. In this example, the Mobitz I second degree AV block (mixed 3:2 and 4:3 Wenckebach behavior with progressively lengthening of AV conduction) is developed at 200s, thus persistent AS-VS rhythm cannot be maintained. Nonetheless, the repetitive AV hysteresis allows pacer continue operate (repetition) at long AV delay (for up to 5 cycles) even if one VP occurs. Therefore, although VPs are delivered due to intermittent AV block, many intrinsic AV conductions are preserved by the repetitive AV hysteresis.

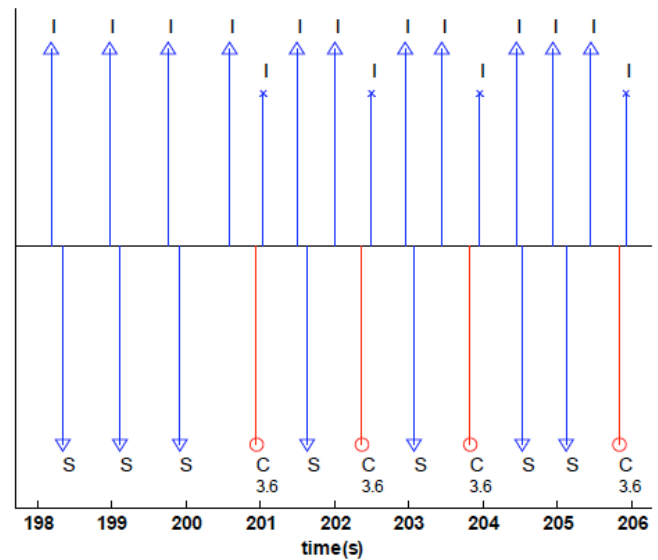


Fig. (18). An exemplary segment of model-generated event markers for applying repetitive AV hysteresis in the presence of second degree AV block. Reprinted from [24] with permission (© 2009, IEEE).

V. FUTURE STUDIES

The IDHP model is an extension of the previous AF-VP model, [11] which is further built upon the AF model developed by Cohen *et al.* [4]. Further improvement of the model is certainly warranted. The open source releases of the AF-VP model in PhysioNet and the IDHP model in Physiome will encourage the usage and enhancement of these models. We hope this open access description of the IDHP model, along with the open access paper on AF-VP model, [18] will further strengthen and accelerate research collaborations in the field.

The IDHP model provides an abstract representation of the native cardiac electrical conduction system and its interactions with the external cardiac pacing. One unique feature of the model is that its software architecture is constructed in a modular manner. This modular design not only facilitates model change for achieving a particular purpose (e.g., to simulate a new ARG model with different statistical properties), but also allows potentially more realistic features of the heart and device to be encapsulated into respective modular units. For example, it has been recognized that the AV conduction not only depends on the recovery time, but also is affected by the autonomic modulation [25-27]. Other nonlinear dynamics of the AV conduction under specific conditions were also reported, such as alternans [28] and hysteresis [29, 30]. All these realistic features can be incorporated within the same model framework, by choosing different formulas to characterize the AV conduction time and the AVJ refractory period.

Moreover, the pacer module can be customized to simulate various timing control logics that are specific to different pacemaker models, and many advanced pacing algorithms can be easily incorporated into the model as exemplified in Figs. 16-18. Besides PMT and 2:1 lock-in (see Fig. 13 and Fig. 14), many other device-related issues frequently encountered in clinics (e.g., over-sensing, under-sensing, feature interactions, etc.) can be simulated, which may not only facilitate root-cause analysis, but also guide the development of new pacemaker features to correct these misbehaviors or mitigate the associated risks. Hence, the IDHP model provides a unique simulation environment, which makes it possible to rigorously bench test new pacemaker algorithms (in the presence of different heart rhythms) even before experimental or clinical investigations, thus may speed up the development of novel device features for cardiac rhythm management.

Finally, in view of the rapid progress in cardiac resynchronization therapy for treating refractory heart failure with cardiac dyssynchrony, [31] the next incremental step to build an integrated three-chamber (right atrium, right ventricle, left ventricle) heart and pacer model will be both challenging and rewarding.

REFERENCES

- [1] Mond HG, Irwin M, Morillo C, Ector H. The world survey of cardiac pacing and cardioverter defibrillators: calendar year 2001. *Pacing Clin Electrophysiol* 2004; 27:955-64.
- [2] Malik M, Camm AJ. Heart rate variability. Armonk: Futura 1995.
- [3] Chorro FJ, Kirchhof CJ, Brugada J, Allessie MA. Ventricular response during irregular atrial pacing and atrial fibrillation. *Am J Physiol* 1990; 259: H1015-21.
- [4] Cohen RJ, Berger RD, Dushane TE. A quantitative model for the ventricular response during atrial fibrillation. *IEEE Trans Biomed Eng* 1983; 30: 769-81.
- [5] Honzikova N, Fiser B, Semrad B. Ventricular function in patients with atrial fibrillation. A simulation model study with the aid of a computer. *Cor Vasa* 1973; 15: 257-64.
- [6] Jorgensen P, Schafer C, Guerra PG, Talajic M, Nattel S, Glass L. A mathematical model of human atrioventricular nodal function incorporating concealed conduction. *Bull Math Biol* 2002; 64: 1083-99.
- [7] Meijler FL, Jalife J, Beaumont J, Vaidya D. AV nodal function during atrial fibrillation: the role of electrotonic modulation of propagation. *J Cardiovasc Electrophysiol* 1996; 7: 843-61.
- [8] Moe GK, Abildskov JA. Observations on the ventricular dysrhythmia associated with atrial fibrillation in the dog heart. *Circ Res* 1964; 14: 447-60.
- [9] Talajic M, Papadatos D, Villemaire C, Glass L, Nattel S. A unified model of atrioventricular nodal conduction predicts dynamic changes in Wenckebach periodicity. *Circ Res* 1991; 68:1280-93.
- [10] Zeng W, Glass L. Statistical properties of heartbeat intervals during atrial fibrillation. *Phys Rev E* 1996; 54: 1779-84.
- [11] Lian J, Mussig D, Lang V. Computer modeling of ventricular rhythm during atrial fibrillation and ventricular pacing. *IEEE Trans Biomed Eng* 2006; 53: 1512-20.
- [12] Lian J, Mussig D, Lang V. Ventricular rate smoothing for atrial fibrillation: a quantitative comparison study. *Europace* 2007; 9: 506-13.
- [13] Lian J, Mussig D, Lang V. On the role of ventricular conduction time in rate stabilization for atrial fibrillation. *Europace* 2007; 9: 289-93.
- [14] Lian J, Mussig D, Lang V. Validation of a novel atrial fibrillation model through simulated atrial pacing protocols. *Conf Proc IEEE Eng Med Biol Soc. New York City* 2006; pp. 4024-7.
- [15] Lian J, Mussig D. Heart rhythm and cardiac pacing: an integrated dual-chamber heart and pacer model. *Ann Biomed Eng* 2009; 37: 64-81.
- [16] Goldberger AL, Amaral LA, Glass L, *et al.* PhysioBank, PhysioToolkit, and PhysioNet: components of a new research resource for complex physiologic signals. *Circulation* 2000; 101: E215-20.
- [17] Hunter P, Robbins P, Noble D. The IUPS human Physiome Project. *Pflugers Arch* 2002; 445: 1-9.
- [18] Lian J, Clifford G, Mussig D, Lang V. Open source model for generating RR intervals in atrial fibrillation and beyond. *BioMed Eng OnLine* 2007; 6: 9.
- [19] Heethaar RM, De Vos Burchart RM, Denier Van Der Gon JJ, Meijler FL. A mathematical model of A-V conduction in the rat heart. II. Quantification of concealed conduction. *Cardiovasc Res* 1973; 7: 542-56.
- [20] Heethaar RM, Denier van der Gon JJ, Meijler FL. Mathematical model of A-V conduction in the rat heart. *Cardiovasc Res* 1973; 7: 105-14.
- [21] Ellenbogen KA, Wood MA. Cardiac Pacing and ICDs. Malden: Blackwell Publishing 2005.
- [22] Goethals M, Timmermans W, Geelen P, Backers J, Brugada P. Mode switching failure during atrial flutter: the '2:1 lock-in' phenomenon. *Europace* 2003; 5: 95-102.
- [23] Lian J, Mussig D, Lang V. Adaptive ventricular rate smoothing during atrial fibrillation: a pilot comparison study. *Conf Proc IEEE Eng Med Biol Soc. Shanghai: IEEE* 2005, pp. 3881-4.
- [24] Lian J, Garner G, Krätschmer H, Müssig D. simulation of AV hysteresis pacing using an integrated dual chamber heart and pacer model. *Conf Proc IEEE Eng Med Biol Soc. Minneapolis: IEEE* 2009, pp. 3932-5.
- [25] Leffler CT, Saul JP, Cohen RJ. Rate-related and autonomic effects on atrioventricular conduction assessed through beat-to-beat PR interval and cycle length variability. *J Cardiovasc Electrophysiol* 1994; 5: 2-15.
- [26] Warner MR, deTarnowsky JM, Whitson CC, Loeb JM. Beat-by-beat modulation of AV conduction. II. Autonomic neural mechanisms. *Am J Physiol* 1986; 251: H1134-42.
- [27] Warner MR, Loeb JM. Beat-by-beat modulation of AV conduction. I. Heart rate and respiratory influences. *Am J Physiol* 1986; 251: H1126-33.
- [28] Christini DJ, Stein KM, Markowitz SM, *et al.* Complex AV nodal dynamics during ventricular-triggered atrial pacing in humans. *Am J Physiol Heart Circ Physiol* 2001; 281: H865-72.

- [29] Shenasa M, Lacombe P, Godin D, Sadr-Ameli MA, Faugere G, Nadeau RA. Atrioventricular nodal conduction and refractoriness following abrupt changes in cycle length. *Pacing Clin Electrophysiol* 1988; 11: 1281-90.
- [30] Zhao J, Billette J. Characteristics and mechanisms of the effects of heart rate history on transient AV nodal responses. *Am J Physiol* 1996; 270: H2070-80.
- [31] Abraham WT, Hayes DL. Cardiac resynchronization therapy for heart failure. *Circulation* 2003; 108: 2596-603.

Received: December 18, 2009

Accepted: February 01, 2010

© Lian *et al.*; Licensee *Bentham Open*.

This is an open access article licensed under the terms of the Creative Commons Attribution Non-Commercial License (<http://creativecommons.org/licenses/by-nc/3.0/>) which permits unrestricted, non-commercial use, distribution and reproduction in any medium, provided the work is properly cited.